JOURNAL OF SPACECRAFT AND ROCKETS
Vol. 29, No. 6, November-December 1992

Radiation Exposure Predictions for Short-Duration Stay Mars Missions

Scott A. Striepe,* John E. Nealy,* and Lisa C. Simonsen*
NASA Langley Research Center, Hampton, Virginia 23665

The human radiation environment for several short-duration stay manned Mars missions is predicted using the Mission Radiation Calculation (MIRACAL) program, which was developed at NASA Langley Research Center. This program provides dose estimates for galactic cosmic rays (GCR) and large and ordinary solar proton flare events for various amounts of effective spacecraft shielding (both operational and storm shelter thicknesses) and a given time history of the spacecraft's heliocentric position. The results of this study show that most of the missions can survive the most recent large flares (if they were to occur at the missions' perihelion) if a 25 g/cm^2 storm shelter is assumed. The dose predictions show that missions during solar minima (when solar flare activity is the lowest) are not necessarily the minimum dose cases, due to increased GCR contribution during this time period. The direct transfer mission studied has slightly lower doses than the outbound Venus swingby mission [on the order of 10–20 centi-Sieverts (cSv) lower], with the greatest dose differences for the assumed worst case scenario (when the large flares occur at perihelion). The GCR dose for a mission can be reduced by having the crew spend some fraction of its day nominally in the storm shelter (other than during flare events).

Nomenclature

BFO	= blood-forming organ
CAM	= computerized anatomical man
COSPAR	= Committee on Space Research
GCR	= galactic cosmic rays
NCRP	= National Council on Radiation Protection and Measurements
OP	= operational shield
R	= spacecraft heliocentric distance, AU
SF	= shadow factor
SS	= storm shelter

Introduction

As the next century rapidly approaches, preliminary analyses of manned excursions to Mars are becoming more detailed. The recent report of the Synthesis Group on America's Space Exploration Initiative[1] identified radiation effects and shielding as an area where technology development is required. In an effort to provide the vehicle design engineer with accurate information on crew radiation exposure, a computer program has been developed that quantifies the radiation environment encountered during Mars missions. This study illustrates the use of this new program by analyzing the radiation environments for several short-duration stay class missions.

The short-duration stay missions were selected for this radiation exposure assessment because of several interesting characteristics that they exhibit. These missions typically have less than 100-day stay times at Mars and less than two years total mission duration. Also, these missions generally have a Venus swingby on either the outbound (Earth-Mars) or the inbound (Mars-Earth) transfer; thus, they usually have a perihelion of less than 0.72 AU and an aphelion of at least 1.5 AU. Because of these trajectory characteristics, an incurred dose assessment cannot be based on the particle environment at Earth's 1.0 AU orbit without some compensation for the significantly different perihelion and aphelion distances. Note that these missions also use high thrust propulsion systems [such as nuclear thermal propulsion (NTP) or chemical propulsion systems], but only the radiation exposure due to natural sources (i.e., solar flares and GCR) are estimated using the MIRACAL program.

Presented as Paper AAS 92-107 at the AAS/AIAA Spaceflight Mechanics Meeting, Colorado Springs, CO, Feb. 24–26, 1992; received March 19, 1992; revision received May 6, 1992; accepted for publication May 22, 1992.

*Aerospace Engineer, Space Systems Division.

Background

The mission radiation calculation (MIRACAL) computer program,[2,3] which was developed at NASA Langley Research Center, uses a comprehensive data base that includes extensive information related to the major natural radiation sources for exposure during interplanetary missions. These sources include GCR, very large proton flares (six are included in this data base), and smaller (or ordinary) proton flares. For each of the environmental sources, the data base includes dose versus depth functions, which give the dose equivalent variation in slabs of water (up to a thickness of 30 cm). Dose equivalent values given by MIRACAL are expressed in système international (SI) units of centi-Sieverts, which are numerically equivalent to rem units. Although not used in this study, this program can also provide estimates of the energetic particle fluences encountered (used to analyze radiation exposure in detailed vehicle configurations).

Dose versus depth functions are also included in the data base using the computerized anatomical man (CAM) model[4] for more detailed dose estimates to the skin, ocular lens (eye), and BFOs. The slab model doses are more conservative and larger than doses for the CAM model. The CAM model is considerably more detailed than the slab model, but the MIRACAL program can generate dose estimates for either model. More details on the differences between these two models can be found in Ref. 3.

The slab dose versus depth functions for the GCR, large flares, and ordinary flares used in MIRACAL are shown in Figs. 1, 2, and 3, respectively. These dose functions are based on detailed radiation transport calculations performed with the NASA Langley nucleon and heavy ion transport codes, BRYNTRN[5] and HZETRN.[6] Effects of energy transfer due to primaries and secondary particles are accounted for, and dose equivalent has been evaluated according to the presently accepted quality factors recommended by the International

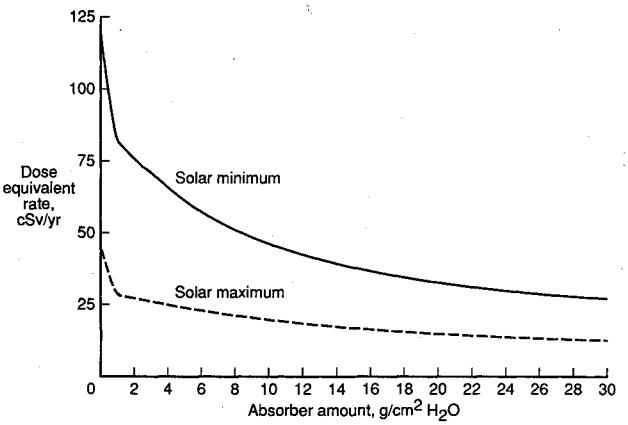

Fig. 1 Depth-dose functions (GCR).

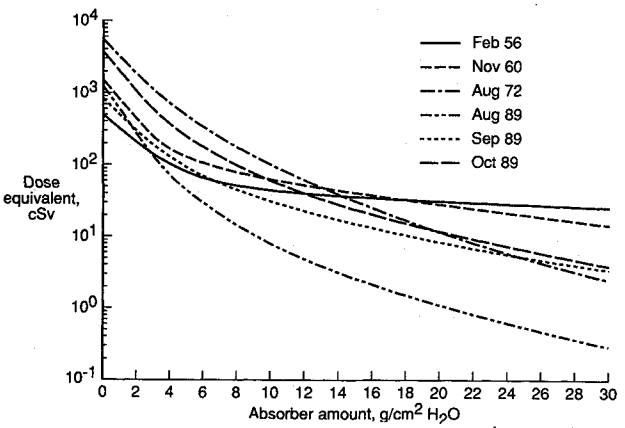

Fig. 2 Depth-dose functions (large flares).

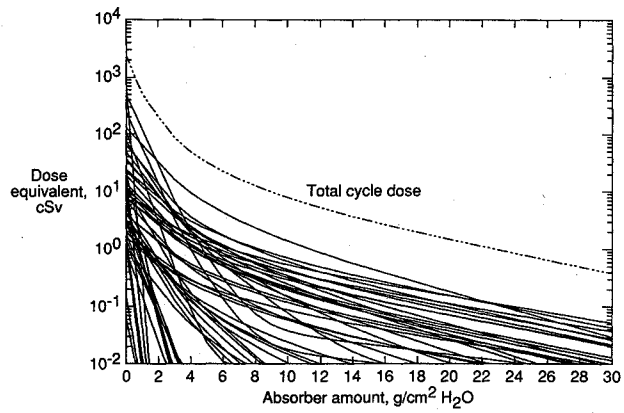

Fig. 3 Depth-dose functions (ordinary flares).

Commission on Radiological Protection.[7] The three figures show either the dose equivalent (in cSv) or its rate (in cSv/yr) versus the amount of the absorber in g/cm^2 of water. The absorber amount is given in terms of a density thickness (g/cm^2), which is determined from the density of the material (g/cm^3) multiplied by its thickness (cm). Thus, shields of equal density thickness have equal masses, though their linear thickness may differ.

In Fig. 1, the GCR conditions at solar minimum and maximum are shown; solar minimum occurs during the first and last few years of the 11-year solar cycle, when the solar activity is at a minimum. Since the interplanetary magnetic field is strongest at solar maximum, more of the intergalactic particles (which are constituents of the GCR) are deflected than during solar minimum; thus, the GCR contribution to the incurred dose is greatest at solar minimum. Particle fluxes (used to calculate the dose equivalent values) for the GCR use the Naval Research Laboratory CREME model for solar minimum and maximum conditions.[8] The modulation of the GCR fluxes between solar minimum and maximum extrema is incorporated using a weighting function derived from the intensity of the 10.7-cm radiance (F10.7) solar activity index, as observed during solar cycle XXI (1975–1986).[3] For the GCR dose contributions, the dose variation as a function of time after the last solar minimum is then determined for an 11-year cycle.

The incurred dose at 1 AU for the large and ordinary flares are shown in Figs. 2 and 3, respectively. The six large proton events recorded in the last four solar cycles are represented in Fig. 2. The spectra of the February 1956 and November 1960 flares were extrapolated from either ground-based sensors or sounding rocket data and, therefore, may be extremely conservative and less reliable. The last four flares were measured using space-based instruments and are considered more accurate. The distinguishing characteristic between large and ordinary flares (as defined for the MIRACAL code)[2,3] is that the delivered dose of each of the large flares is on the order of the

Table 1 Inputs to the MIRACAL program

Time history of spacecraft heliocentric position.
Periapse and apoapse radius of Mars parking orbit.
Type of calculation desired (fluence, dose, fluence, and dose).
Ordinary flare model type (statistical or smeared).
Number of large flares occurring during the mission (0–6).
Large flare spectrum to use in calculations (Feb. 56, Nov. 60, Aug. 72, Aug. 89, Sept. 89, Oct. 89).
Times of occurrence of large flares (in mission elapsed time).
Operational shielding amount (0–25 g/cm^2 water slabs).[a]
Storm shelter shield amount (0–25 g/cm^2 water slabs).[a]
Percent crew time nominally spent in the storm shelter (daily fraction).

[a]Note that the OP is around the astronauts during regular activities, whereas the storm shelter is only used during solar proton flare events, unless specified otherwise. Additionally, these shieldings are not additive; that is, the total effective shielding is input for both types. For example, 2 g/cm^2 operational and 20 g/cm^2 storm shelter thicknesses do *not* provide 22 g/cm^2 effective shielding while in the storm shelter.

Table 2 Sample MIRACAL output

Earth departure date	53167.00
Venus departure date	53327.00
Mars arrival date	53472.00
Mars departure date	53502.00
Earth Arrival date	53687.00
ra = 3680.00	
rp = 3680.00	
SF = 0.69774	
This is a dose calculation	
Smeared model used for ordinary flares	
No. of large flares = 1	
Calc begins at year 7.480581 in cycle	
OP = 4 g/cm^2	
SS = 20 g/cm^2	
with 33.3 percent time in shelter	
Large flare type 3 at year 7.809348	
Mission total doses, cSv:	
Slab doses—	
Ordinary flares:	0.355 0-cm; 0.178 5-cm
Large flares:	40.953 0-cm; 17.457 5-cm
GCR:	58.591 0-cm; 45.529 5-cm
Total accumulated:	99.898 0-cm; 63.164 5-cm
Highest 30-day dosage:	44.152 0-cm; 19.945 5-cm starting day 120
Highest annual dosage:	83.294 0-cm; 50.225 5-cm starting day 120
CAM model doses—	
Ordinary flares (skin, eye, BFO):	0.214 0.216 0.097
Large flares (skin, eye, BFO):	23.663 23.579 9.404
GCR (skin, eye, BFO):	47.219 47.555 37.733
Total accumulated (skin, eye, BFO):	71.096 71.350 47.234
Highest 30-day dosage (skin, eye, BFO):	26.241 26.176 11.464 starting day 120
Highest annual dosage (skin, eye, BFO):	57.694 57.851 36.505 starting day 120

total dose of all of the ordinary flares combined. All 55 ordinary flares used in the MIRACAL program occurred in solar cycle XXI and are shown in Fig. 3. In each of these figures, the dose equivalent is reduced as more absorber material is added, as one would expect.

Various detailed or parametric studies can be made using the MIRACAL program. This code allows variation of the nominal vehicle shielding thickness, flare storm shelter thickness, nominal time spent in the storm shelter (other than during a large proton event), the type of large flare environment, and the time during the mission at which large proton events may occur (Table 1 summarizes the required MIRACAL inputs). Since a time history of the spacecraft's heliocentric position is required as input, any mission type can be simulated using this routine. This program assumes a $1/R^2$ dependence for all flares encountered (both ordinary and large proton events), where R is the spacecraft's heliocentric distance (in AU). Additionally, planetary shielding is taken into account when the spacecraft is in orbit about a planet. An average shadow factor (SF), calculated from the periapse and apoapse of the parking orbit, indicates the percentage of flare or GCR dose that reaches the astronauts while in orbit; an astronaut standing on the surface of a planet with no atmosphere receives only 50% of the normal dose (SF = 0.5), whereas an astronaut in a parking orbit of sufficient height would receive the entire normal dose (SF = 1.0), or no planetary shielding. Shielding due to the Martian atmosphere can also be accounted for during crew surface stays. Table 2 shows a sample of the output generated by the MIRACAL code.

The algorithm estimates the incurred dose rate variation as a function of mission elapsed time. This data allows the evaluation of the highest annual (365-day), 30-day, and total dosage received during the mission. Considering the NCRP-recommended guidelines on the dosage received during these time periods (see Table 3, taken from Ref. 9), the design engineer can evaluate various combinations of storm shelter thickness, nominal time spent in the shelter, and alteration of the interplanetary trajectory necessary in order not to exceed those limits.

The Mars surface doses presented in this analysis are calculated using the methodology of Ref. 10. The amount of protection provided by the Mars atmosphere against GCR and solar proton flares will depend on the composition and structure of the atmosphere as well as the crew members' altitude. The current estimates use the COSPAR low-density model of the Martian atmosphere (5.9 mb surface pressure)[11] and assume a 100% carbon dioxide composition. All calculations are for an altitude of 0 km on the Martian surface. A spherically concentric atmosphere is used such that the amount of protection provided overhead varies from approximately 16 g CO_2/cm^2, increasing to 59.6 g/cm^2 at large zenith angles. All surface dose estimates consider the atmosphere as the crew's only protection and do not take into account any additional shielding provided by their pressure vessel and supporting equipment or supplies. Analyses have shown that moderate thicknesses of additional shielding do not provide substantial protection in addition to that already provided by the carbon dioxide atmosphere.[12]

Table 3 NCRP dose equivalent limit guidelines,[9] cSv

	Skin	Eye	BFO
30-day	150	100	25
Annual	300	200	50
Career	600	400	100–400[a]

[a]Age and gender dependent.

Approach

In this study, the radiation exposure incurred during several of the short-duration stay class missions, which have been suggested for manned Mars missions in the first part of the next century, has been estimated. These missions, presented in Table 4 and Fig. 4, are taken from Refs. 13–21. Both the table and the figure indicate the Mars stay time (above the mission box in Fig. 4) and the total mission time (below the mission box) in days. These 12 missions have Earth departure dates ranging from 2004 to 2023. Since the solar cycle is approximately 11 years in duration, this range of Earth departure dates permits examination of missions throughout a couple of solar cycles. (See Fig. 4.) Additionally, most of these missions pass well inside Venus' orbit, thus providing an opportunity to assess the radiation environment predicted for these types of missions.

Because of the extremely unpredictable nature of the large proton flare events, several large flare scenarios were examined. One scenario (the best case) estimates the mission's radiation exposures if no large flares were to occur. We define our worst case scenario as one that has a major flare occur at the perihelion of the interplanetary transfer. Since the type of flare that might occur is very unpredictable, each large flare was used in our worst case assessments; that is, only one flare at mission perihelion was evaluated for each of the six worst cases studied. Additionally, a scenario is included in which the September 1989 large flare is assumed to have occurred during the surface stay of each mission. Except for this scenario, the doses are calculated for the crew in orbit during the entire stay time at Mars; that is, Mars atmospheric shielding is only used in the surface flare scenario. The other scenarios assume the more conservative case where the astronaut remains in orbit, outside atmospheric protection, during the entire Mars stay. For the ordinary flare dose contributions, a smeared, or averaged, model is used throughout the missions.

Table 4 Dates and data for short-duration stay missions studied

	Mission dates						Mission data				
							At Mars		Interplanetary Transfer		Ref. No.
Mission title	Earth departure	Outbound Venus swingby	Mars arrival	Mars departure	Inbound Venus swingby	Earth return	Stay time, days	Shadow factor	Trip time, days	Perihelion radius, AU	
2004	10 June 2004	17 Nov. 2004	11 April 2005	11 May 2005		12 Nov. 2005	30	0.70	520	0.58	13
2007	30 Aug. 2007		15 Feb. 2008	26 March 2008	4 Oct. 2008	22 March 2009	40	0.99	570	0.56	[a]
2011	6 Jan. 2011	12 May 2011	27 Sept. 2011	27 Oct. 2011		20 May 2012	30	0.99	500	0.52	14
2014-A	17 Jan. 2014		11 July 2014	19 Oct. 2014	28 Feb. 2015	26 July 2015	100	0.98	555	0.56	15
2014-B	15 Jan. 2014		27 Aug. 2014	26 Sept. 2014	23 Feb. 2015	14 July 2015	30	0.75	545	0.55	16
2014-C	1 Feb. 2014		1 July 2014	29 Sept. 2014	26 Feb. 2015	5 Aug. 2015	90	0.75	550	0.56	17
2016-D	1 Oct. 2016		26 Feb. 2018	27 April 2018		1 Oct. 2018	60	0.99	730	1.00	18
2016-I	12 March 2016		4 Aug. 2016	23 Sept. 2016	13 March 2017	11 May 2017	50	0.75	425	0.63	19
2017-D	7 Dec. 2017		13 July 2018	11 Sept. 2018		12 May 2019	60	0.99	521	0.76	20
2017-O	5 April 2017	10 Sept. 2017	24 March 2018	23 May 2018		15 Nov. 2018	60	0.99	589	0.57	18
2020	29 July 2020		18 Nov. 2020	18 Dec. 2020	4 Aug. 2021	30 Jan. 2022	30	0.99	550	0.59	21
2023	2 Sept. 2023	14 Feb. 2024	11 June 2024	10 Aug. 2024		20 May 2025	60	0.99	626	0.53	20

[a]Mission taken from K. Joosten presentation to Nuclear Regulatory Commission Aeronautics and Space Engineering Board on April 30, 1991.

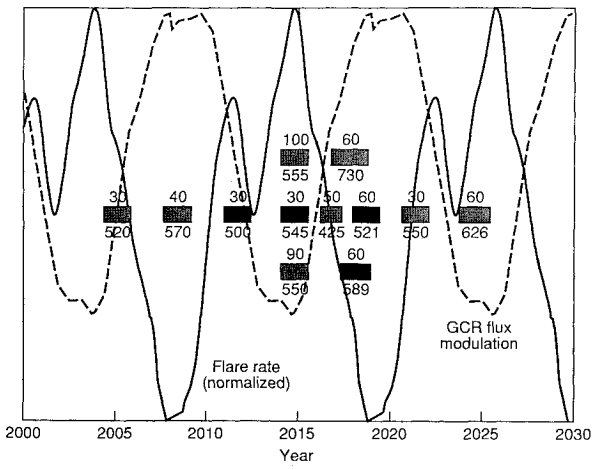

Fig. 4 Candidate Mars missions during three solar cycles.

As just noted, the occurrence of the September 1989 proton flare is considered as a possible scenario during the Mars surface stay. The dose contribution for this proton event is approximately midway between the estimated doses for the August 1989 and October 1989 flare events. The smeared ordinary flare contribution is not considered for the short-duration stay on the surface. The dose contribution with the large amount of atmospheric protection would be negligible (<0.05 cSv), as indicated by the total cycle dose-depth curve in Ref. 3. The skin and eye CAM doses are approximated as the 0-cm depth dose (slab skin), which is conservative in both instances. The CAM BFO dose is conservatively approximated by the 5-cm depth dose (slab BFO). Because of the large amounts of carbon dioxide traversed and the resulting relatively low surface exposures, the additional complexity introduced by the CAM calculations is not warranted for the short-duration stay times.

In this analysis, three operational (OP) thicknesses, four storm shelter thicknesses, and three nominal times in the storm shelter were evaluated. The OP thicknesses, considered to surround the astronauts during normal activities, are 2, 4, and 6 g/cm^2 of water; whereas the storm shelter, which protects the astronauts during solar flares (both large and ordinary flares), has thicknesses of 10, 15, 20, and 25 g/cm^2 of water. Also, the option of having the crew spend some fraction of the day in the storm shelter, other than during flare events (in order to lower the GCR dose contribution), was investigated. For this study, the nominal times in the storm shelter are one-third and one-half a day. Also, the missions were evaluated assuming no time nominally spent in the storm shelter.

Results

As seen in Fig. 4, the missions selected for study encounter vastly different GCR and solar flare environments. This section will begin with the required OP and storm shelter shielding thickness necessary for each mission to remain below the NCRP-suggested guideline limits shown in Table 3. Results for 12 missions are included; however, four missions are examined more closely: the 2011, 2014-B, 2017-D, and 2017-O missions (the four darkest boxes in Fig. 4). The first three cases permit analysis of missions that primarily occur during solar minimum, solar maximum, or between these two extremes. The 2017 missions will indicate some of the differences, in terms of radiation exposure, between a direct and an outbound Venus swingby mission. The effect of changing the crews nominal time spent in the storm shelter is studied next. Finally, an assessment of the impact that the surface flare scenario has on the missions is considered.

Table 5 shows the OP and storm shelter shielding thickness requirements for each mission to meet the NCRP slab dose guidelines for BFOs when the scenarios using the four latest large flares (August 1972 and August, September, and October 1989) are considered the worst case. Since the protection of the BFO often dictates shield thickness requirements, the slab BFO guideline limit was selected as the main criterion to ensure that all NCRP guidelines would be satisfied. The table includes the minimized OP and storm shelter thickness cases since the size of the storm shelter, in comparison to the overall vehicle, is unknown. If the storm shelter is much smaller than the vehicle, then the minimum OP case is used because the total vehicle mass will be smaller; conversely, when the storm shelter occupies an appreciable volume of the vehicle, the minimum storm shelter case would have the least amount of total vehicle mass.

Over half of the missions studied can satisfy the NCRP requirements with no additional time spent in the storm shelter (beyond retreating to the shelter during a flare event). As the nominal crew time in the storm shelter is increased to one-half, all but one mission can meet the slab BFO guideline limits using the thicknesses analyzed in this study. The 2007 mission exceeds the slab BFO annual guideline limit by 0.3 cSv when using a 6 g/cm^2 OP and 25 g/cm^2 storm shelter thicknesses. None of the missions had enough shielding to protect against the worst case scenarios involving the first two major flares recorded (February 1956 and November 1960). Almost all of the missions require the 25 g/cm^2 storm shelter, whereas a majority of the missions only needs the 2 g/cm^2 OP thickness.

In order to study the effect that the solar cycle has on a mission's radiation exposure, three missions are selected for further analysis: one at solar maximum (2014-B); one in between the extrema (2011); and one at solar minimum (2017-D). The location of these three missions during the solar cycle is indicated by the darkest boxes in Fig. 4 (2017-D is above 2017-O). Additionally, to permit an even comparison, the 4 g/cm^2 OP and 20 g/cm^2 storm shelter thickness cases were arbitrarily selected for study.

The incurred doses for these three missions, having the aforementioned shielding thicknesses, are shown in Figs. 5–7. In these figures, all of the flare scenarios are included. Note that these three plots have a logarithmic ordinate axis. For the cases with large flares at perihelion, the 30-day maximum dose is driven by the large flare dose contribution; thus, this dose is also indicative of the large flare dose. The lines across the plot indicate the NCRP guideline 30-day and annual limits for skin and BFO (see Table 3). The 0-cm depth-dose (used to approximate dose to both skin and eye) and the 5-cm depth-dose (used to approximate dose to BFO) are shown for each scenario, as well as the CAM-modeled skin, eye, and BFO dose estimates.

Table 5 Minimum combination of examined thicknesses required to meet NCRP slab BFO guideline limits for recent large flare, worst case scenarios

	Amount of crew time nominally spent in SS											
	Zero				One-third				One-half			
	Min OP g/cm^2		Min SS g/cm^2		Min OP g/cm^2		Min SS g/cm^2		Min OP g/cm^2		Min SS g/cm^2	
Mission title	OP	SS	OP	SS	OP	SS	OP	SS	OP	SS	OP	SS
2004	6	25	6	25	2	25	2	25	2	25	2	25
2007	N[a]	N	N	N	N	N	N	N	N	N	N	N
2011	N	N	N	N	6	25	6	25	2	25	2	25
2014-A	2	25	2	25	2	25	2	25	2	25	2	25
2014-B	2	25	2	25	2	25	2	25	2	25	2	25
2014-C	2	25	2	25	2	25	2	25	2	25	2	25
2016-D	4	25	6	10	2	15	4	10	2	10	2	10
2016-I	6	25	6	25	2	25	2	25	2	25	6	20
2017-D	N	N	N	N	6	25	6	25	2	25	2	25
2017-O	N	N	N	N	N	N	N	N	6	25	6	25
2020	N	N	N	N	N	N	N	N	4	25	4	25
2023	2	25	2	25	2	25	2	25	2	25	2	25

[a]N = Thickness required for OP>6 g/cm^2 and SS>25 g/cm^2.

In Fig. 5, the predicted dose for the 2014-B mission occurring mostly during solar maximum is shown. The no flare case easily meets all of the NCRP guideline limits. However, the first two large flares greatly exceed the BFO limits. Of the remaining flare cases, only the October 1989 flare forces the mission to exceed the BFO limits. To facilitate solar cycle mission comparisons, concentrate on the no flare case. Note that the no flare scenario has a mission total slab skin dose of about 60 cSv and a BFO dose of around 45 cSv. When compared to the mission occurring mostly between the solar cycle extrema regions in Fig. 6, the no flare slab skin and BFO total dose rise to a little more than 70 cSv and 50 cSv, respectively. This increase can be attributed to the increased GCR flux during times of solar minimum conditions. Also, although the 30-day BFO limit is exceeded only during the October 1989 flare scenario (considering only the four most recent flares) for this mission, the doses for the large flare cases are greater than for the previous mission (approaching the 25 cSv limit). This fact is due not only to the increased contribution of the GCR, but also to the lower perihelion radius of the 2011 mission (0.03 AU closer to the sun).

For the 2017-D mission, which occurs mostly at solar minimum, Fig. 7 indicates that the no flare scenario total slab dose

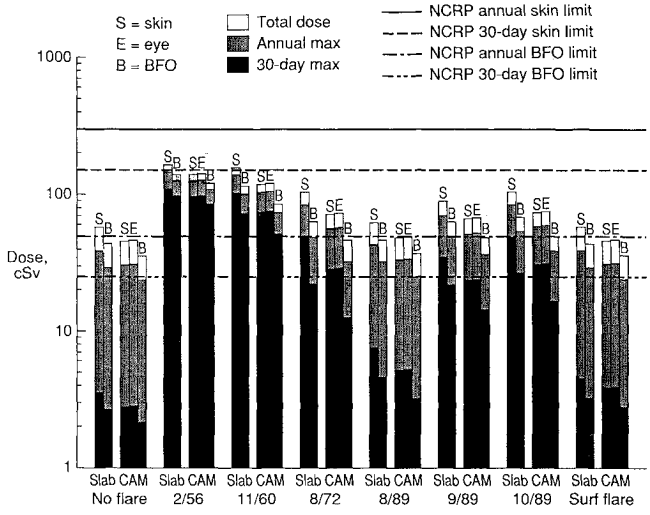

Fig. 5 Radiation exposure for mission during solar maximum—2014-B inbound Venus swingby.

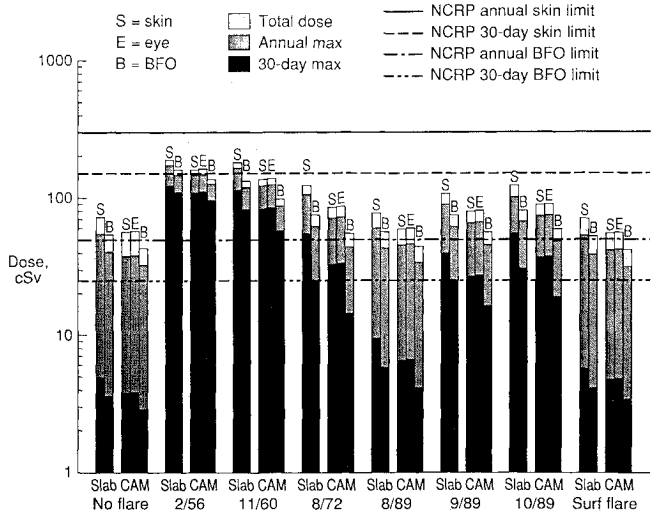

Fig. 6 Radiation exposure for mission between solar cycle extrema—2011 outbound Venus swingby.

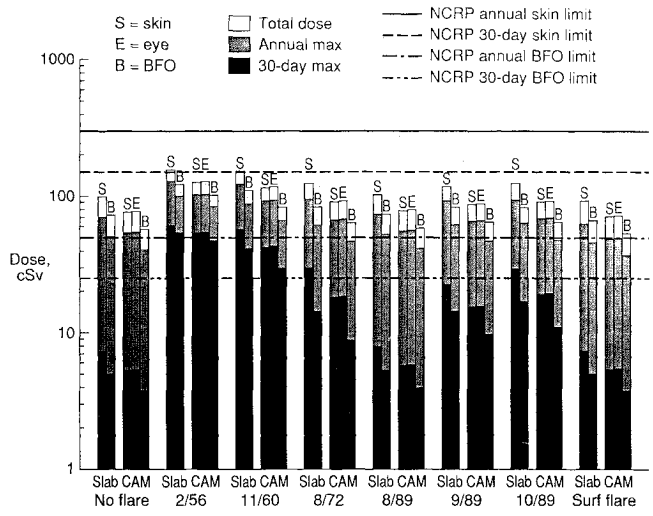

Fig. 7 Radiation exposure for mission during solar minimum—2017 direct transfer.

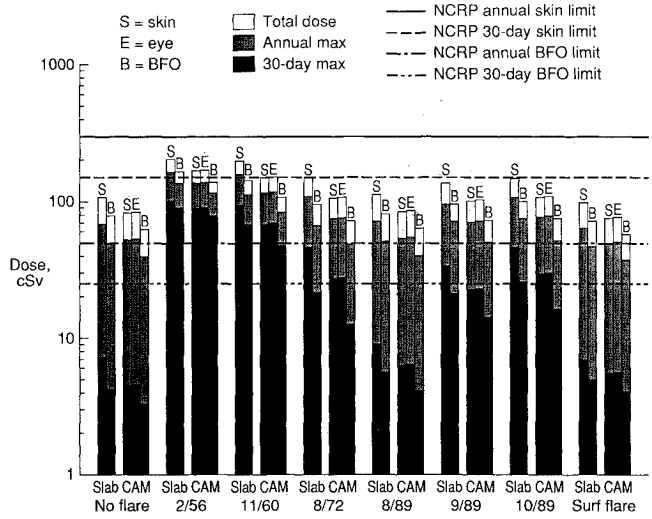

Fig. 8 Radiation exposure for 2017 outbound Venus swingby mission.

is nearly 100 cSv for the skin and 70 cSv for the BFO; again, this increased dosage can be attributed to the larger GCR dose contribution. Additionally, Fig. 7 shows that whereas none of the 30-day BFO limits is exceeded for the most recent flares, all of the annual limits are violated. The lower 30-day maximum is due more to the larger perihelion radius of the 2017-D mission (about 0.21 AU further out than the 2014-B mission), whereas the slightly increased annual dose amounts show the long-term effect of the increased GCR dose. From this analysis, missions at solar maximum appear to encounter a more favorable environment when no flares occur; however, the greatest probability of a large flare occurring is during the solar maximum period.

Whereas Fig. 7 plots the predicted dose for a direct Earth-Mars mission beginning in 2017, Fig. 8 depicts the dose for a mission with an outbound Venus swingby. As indicated by the darkest boxes around 2017 in Fig. 4, these missions both occur during approximately the same time frame (again, 2017-D is above 2017-O). The main difference in these two missions is the approximately 0.2 AU difference in their perihelion radii (Table 4), which has a greater effect on the doses of the large flare cases, as illustrated by Figs. 7 and 8. The 30-day maximum doses for the worst case scenarios, which are driven by the dose contributed by the large flare, are higher for the outbound Venus swingby mission because of its lower peri-

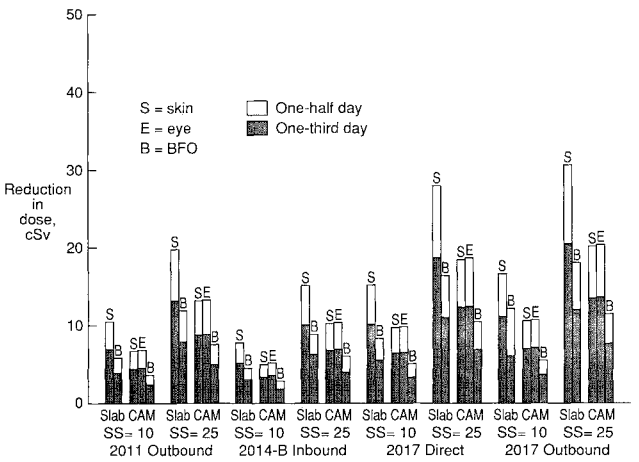

Fig. 9 GCR dose reduction from increased nominal time in storm shelter.

helion. The no flare case has only a few cSv increase in the 30-day and annual maximum doses for the outbound swingby mission; the total dose for both slab and CAM models in this scenario is less than 10 cSv higher for the swingby mission. The scenarios with the 1972 and 1989 flares generally have 30-day maximum, annual maximum, and total doses 10–20 cSv higher for the swingby mission. Thus, the difference in the radiation received for direct and Venus swingby missions is not as great as might be expected.

The radiation exposure due to GCR can be reduced by the crew spending more time in the storm shelter other than during solar flare events. Figure 9 shows the effect of increased nominal time spent in the storm shelter for the four missions previously mentioned. The mission at solar maximum (2014-B) is least affected by the additional time spent in the storm shelter; whereas the effect is greatest on the missions at solar minimum (2017-D and 2017-O) due to the greater contribution of the GCR to the total dose. As seen in Fig. 9, if one-third of an astronaut's day (equivalent to an eight-hour sleep period) is spent in a 10 g/cm^2 storm shelter, the reduction in the total dose ranges from about 5 to more than 10 cSv for slab and from around 3 to almost 8 cSv for CAM doses. However, if the time is increased to one-half day, these doses are additionally reduced by about 33%, with the slab dose savings of almost 20 cSv and the CAM dose reduced by a little more than 10 cSv. When a 25 g/cm^2 storm shelter is used, the dose reduction nearly doubles. The dose reductions for one-third day in the storm shelter are now from a little less than 10 cSv to a high of more than 20 cSv using the slab model and from about 5 cSv to about 13 cSv for the CAM dose. If the time spent in the shelter is increased to one-half day, the reduction in dose increases to more than 30 cSv for slab skin, almost 20 cSv for slab BFO and CAM skin, and more than 10 cSv for CAM BFO. Thus, for some missions that violate the NCRP guideline dose limits, simply requiring that the sleep period of the astronauts be spent in the storm shelter can reduce the radiation exposure to the crew below these guideline limits.

The doses incurred during the surface flare scenario for each of the previously discussed four missions can be found in Figs. 5–8. Note that even though the 30-day maximum for this scenario (September 1989 flare dose at the beginning of the Mars surface stay) is slightly greater than for the no flare scenario, the total doses are approximately the same. This result indicates that the Martian carbon dioxide atmosphere provides substantial protection for the astronauts while they are on the surface; apparently, the atmosphere (and the 0.5 SF provided by the planet) gives more protection than the OP or storm shelter shielding on the interplanetary transfer vehicle. Also notice that each of these four missions meets the NCRP BFO guideline limits.

Conclusions

This study demonstrated the use of the MIRACAL by estimating the incurred dose of 12 short-duration stay manned Mars missions proposed for early in the next century. This code is now available and can be easily integrated into or used with interplanetary trajectory analysis codes. Three OP and four SS thicknesses were examined for their effectiveness in protecting the crew from the radiation environment predicted using MIRACAL. Seven of the 12 missions meet the NCRP guideline slab BFO (5-cm depth) limits for worst case scenarios involving the four most recent large flares (August 1972 and August, September, and October 1989) and having no time nominally spent in a 25 g/cm^2 SS. By increasing this nominal time in the SS to one-half day, 11 of the missions meet the NCRP BFO guidelines, whereas nine missions meet the guidelines if one-third day (or an eight-hour sleep cycle) is nominally spent in the SS. The missions that occur primarily during solar minimum (quiet sun; i.e., when the sun is having little or no flare activity) are not necessarily the lowest dose cases due to the increased GCR contribution during this time period. The 2017 direct transfer mission had only a slightly lower dose than the 2017 outbound Venus swingby mission (the total dose for these missions differed by only 10–20 cSv), with the worst case (large flare) scenarios being affected the most due to the different perihelion radii; thus, direct missions do not necessarily have substantially lower doses than swingby missions. By the crew spending some fraction of their day nominally in the SS (other than during flare events), the GCR dose for a mission can be noticeably reduced. Finally, the Martian atmosphere appears to provide sufficient shielding during a crew surface stay.

References

[1]Stafford, T. P., *America at the Threshold,* Report of the Synthesis Group on America's Space Exploration Initiative, U. S. Government Printing Office, Washington, DC, May 1991.

[2]Nealy, J. E., Simonsen, L. C., and Striepe, S. A., "Space Exploration Mission Analyses for Estimates of Energetic Particle Fluence and Incurred Dose," *Proceedings of the Ninth Symposium on Space Nuclear Power Systems,* AIP Conference Proceedings 246, American Institute of Physics, Albuquerque, NM, Jan. 1992.

[3]Nealy, J. E., Striepe, S. A., and Simonsen, L. C., "MIRACAL: A Mission Radiation Calculation Program for Analysis of Lunar and Interplanetary Missions," NASA TP-3211, May 1992.

[4]Billings, M. P., and Yucker, W. R., "The Computerized Anatomical Man (CAM) Model," NASA CR-134043, Sept. 1973.

[5]Wilson, J. W., Townsend, L. W., Nealy, J. E., Chun, S. Y., Hong, B. S., Buck, W. W., Lamkin, S. L., Ganapol, B. D., Khan, F., Cucinotta, F. A., "BRYNTRN: A Baryon Transport Model," NASA TP-2887, March 1989.

[6]Wilson, J. W., Chun, S. Y., Badavi, F. F., Townsend, L. W., and Lamkin, S. L., "HZETRN: A Heavy-Ion/Nucleon Transport Code for Space Radiations," NASA TP-3146, Dec. 1991.

[7]Anon., "Recommendations of the International Commission on Radiological Protection," ICRP Publication 26, Pergamon, Oxford, England, UK, Jan. 1977.

[8]Adams, J. H., Jr., Silberberg, R., and Tsao, C. H., "Cosmic Ray Effects on Microelectronics, Pt. I: The Near-Earth Particle Environment," Naval Research Lab., NRL Memorandum Rept. 4506-Pt. I, U.S. Navy, Washington, DC, Aug. 1981.

[9]Anon., *Guidance on Radiation Received in Space Activities,* National Council on Radiation Protection and Measurements, NCRP Publication 98, NCRP Publications, Bethesda, MD, July 1989.

[10]Simonsen, L. C., Nealy, J. E., Townsend, L. W., and Wilson, J. W., "Radiation Exposure for Manned Mars Surface Missions," NASA TP-2979, March 1990.

[11]Smith, R. E., and West, G. S., "Space and Planetary Environment Criteria Guidelines for Use in Space Vehicle Development, 1982 Rev. (Vol. 1)," NASA TM-82478, Jan. 1983.

[12]Simonsen, L. C., Nealy, J. E., Townsend, S. W., and Wilson, J. W., "Space Radiation Shielding for a Martian Habitat," SAE TP Ser. 901346, July 1990.

[13]Anon., "Exploration Studies Technical Report Vol. II," NASA TM-4170, NASA Office of Exploration Technology, Dec. 1989, pp. 4–10.

[14]Anon., "Exploration Studies Technical Report Vol. II," NASA TM-4075, NASA Office of Exploration Technology, Dec. 1988, pp. 2-22.
[15]Woodcock, G., "Space Transfer Concepts and Analysis for Exploration Missions," Seventh Quarterly Review, Boeing Aerospace and Electronics, Huntsville, AL, Aug. 1991, p. 2.11.
[16]Joosten, B. K., Drake, B. G., Weaver, D. B., and Soldner, J. K., "Mission Design Strategies for Human Exploration of Mars," IAF Paper 91-336, Oct. 1991.
[17]Soldner, J. K., and Joosten, B. K., "Mars Trajectory Options for the Space Exploration Initiative," AAS Paper 91-438, Aug. 1991.
[18]Braun, R. D., "The Influence of Interplanetary Trajectory Options on a Chemically Propelled Manned Mars Mission," *Journal of the Astronautical Sciences,* Vol. 38, No. 3, July 1990, pp. 289-310.
[19]Weaver, D. B., "Analysis of the Synthesis Group's Space Resource Utilization Architecture," Exploration Programs Office Document XE-92-002, NASA Johnson Spaceflight Center, Houston, TX, Feb. 1992, p. A-5.
[20]Striepe, S. A., "Effect of Interplanetary Trajectory Options on Entry Velocities at the Earth and Mars Atmospheric Interface," M.S. Thesis, Univ. of Texas, Austin, TX, May 1991.
[21]Soldner, J. K., "Round Trip Mars Trajectories—New Variations on Classic Mission Profiles," AIAA Paper 90-3794, Aug. 1990.

Ernest V. Zoby
Associate Editor